Structural Relaxation in Polystyrene and Some Polystyrene Derivatives

A. Brunacci,[†] J. M. G. Cowie,*[,†] R. Ferguson,[†] J. L. Gómez Ribelles,[‡] and A. Vidaurre Garayo[§]

Department of Chemistry, Heriot-Watt University, Edinburgh, EH14 4AS U.K., and Departamento de Termodinamica Aplicada y Departamento de Fisica Aplicada, Universidad Politécnica de Valencia, P.O. Box 22012, 46071 Valencia, Spain

Received February 29, 1996; Revised Manuscript Received August 13, 1996[⊗]

ABSTRACT: The structural relaxation process in polystyrene and three polystyrene derivatives (*p*-methyl, *p*-chloro, and *p*-hydroxy) at temperatures close to the glass transition temperature has been monitored by differential calorimetric measurements of the heat capacities of the polymers after they were subjected to several different thermal histories. The heat capacity (c_p) data were analyzed in terms of the recent configurational entropy model proposed by Gómez and Monleón, and good agreement was found between the experimental and model-simulated DSC thermograms. The effect of the three para substituents upon the structural relaxation process is also discussed.

Introduction

Many liquid materials can be supercooled to temperatures well below the melting temperature without forming a crystalline lattice. Polymers are good examples of these materials due to the difficulty of packing the polymer chains in an ordered lattice. On further cooling, the glass transition takes place forming a glass with molecular mobility and viscosity near that of a solid but lacking crystalline order. It is well-known that glasses are not in thermodynamic equilibrium. When, after the formation history, a glass is kept at constant environmental conditions, it undergoes a process whereby it tries to reach an equilibrium state.[1,2] This process has been called "structural relaxation"[3] or "physical aging"[4] and is manifested by the evolution of several thermodynamic or physical variables such as specific volume, enthalpy, mechanical modulus or loss tangent, dielectric permittivity, refractive index, etc. One of the techniques more frequently used to study the kinetics of the structural relaxation process is differential scanning calorimetry, DSC, since this is able to follow the evolution of the enthalpy during the structural relaxation process, the "enthalpy relaxation", through the measurement of the heat capacity of the sample.

In the DSC experiment a sample of the glass-forming material is subjected to a thermal history that starts at a temperature T_{upper}, above the glass transition temperature T_g. After cooling at a controlled rate, and usually one isothermal period at a temperature T_a called the aging temperature, for a time t_a called the aging time, the sample is brought to a temperature T_{lower} below T_g and subsequently the heat capacity of the sample is measured during a heating scan from T_{lower} to T_{upper}. This experimental $c_p(T)$ curve contains information about the structural relaxation process that took place during the thermal treatment previous to the measurement and during the measuring scan itself. When the thermal history of the sample consists of only a fast cooling from T_{upper} to T_{lower}, the $c_p(T)$ curve measured on heating shows the glass transition as an increase from the values of c_p characteristic of the glass, $c_{pg}(T)$, to those corresponding to the liquid $c_{pl}(T)$, in a more or less narrow temperature interval and with a shape that depends on the cooling rate. The transition takes place in a temperature interval whose width can be characterized by the parameter ΔT, as shown in Figure 1. When T_a is not too far from the glass transition temperature, the $c_p(T)$ curve shows a peak that overlaps the glass transition (see Figure 1b). Thermal histories that combine high cooling rates and low aging temperatures may produce peaks in $c_p(T)$ on the low-temperature side of the glass transition, that have been called sub-T_g peaks. Both types of behavior have been explained in terms of the evolution of the enthalpy during the heating scan due to the structural relaxation process.[1−3,5−11]

The aim of this work is to study the chain mobility of styrene polymers, having different substituents in the para position of the aromatic ring, through their enthalpy relaxation. The polymers were polystyrene, PS, poly(4-methylstyrene) (PMS), poly(4-chlorostyrene) (PClS), and poly(4-hydroxystyrene) (PHS). The starting point is polystyrene, where −H can be taken to represent the baseline in terms of both interaction strength and steric hindrance. The next step in this series was the replacement of −H by a methyl group, which confers steric hindrance but little extra interaction to the polymer. Only after introducing a chlorine atom are enhanced inter- and intrachain interactions present, and this is maximized by introduction of the hydroxyl group, where hydrogen bonding is possible.

The kinetics of the structural relaxation process, as determined from DSC experiments has been reproduced by means of phenomenological models with fitting parameters. The most widely used are based on the idea of the double dependence of the relaxation times on the temperature and on the departure from equilibrium (characterized by the fictive temperature T_f). We call here the NM model the one proposed by Narayanaswamy[12] and later by Moynihan and his group,[3] and the SH model is the one proposed by Scherer[13] and Hodge.[14] Both models are well-known, and their conception and equations have been reviewed several times (see for instance refs 2, 15, and 16). They contain four adjustable parameters that are usually determined by fitting experimental DSC thermograms. It has been found that different sets of parameters are necessary

[†] Department of Chemistry.
[‡] Departamento de Termodinamica Aplicada.
[§] Departamento de Fisica Aplicada.
[⊗] Abstract published in *Advance ACS Abstracts,* November 1, 1996.

S0024-9297(96)00336-1 CCC: $12.00

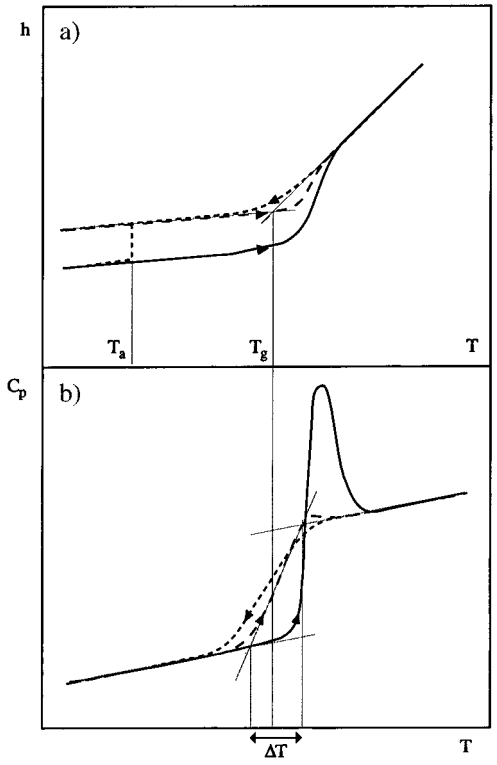

Figure 1. Schematic of the result of the evolution of the enthalpy (a) and heat capacity (b) during a cooling scan through the glass transition region (dotted line), a heating scan performed after it (dashed line), and a heating scan performed after aging at a temperature close to T_g (solid line). The definition of the glass transition temperature is shown in (a) and that of the interval of the glass transition region ΔT in (b).

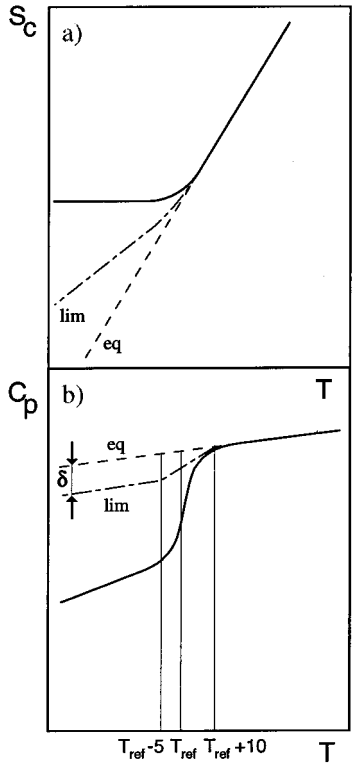

Figure 2. (a) Schematic of the configurational entropy corresponding to the liquid state (dashed line), to an experimental cooling scan at a finite cooling rate (solid line), and to the limit state of the structural relaxation process (dot-dashed line). (b) $c_p(T)$ lines corresponding to the three cases described in (a).

to reproduce accurately the thermograms measured after different thermal histories. Thus the model parameters lose their character of "material parameters" in contradiction with the conceptualization of the model. Several possible causes of this problem have been proposed that refer to the failure of some of the assumptions of these models.[2,15,16] Recently, a model has been proposed[17,18] that introduces a new hypothesis related to the state attained at infinite time in the structural relaxation process at a temperature T_a. This limit state is identified in the NM and SH models with the extrapolation to T_a of the equilibrium line experimentally determined above T_g.[3,12−14] This is simply a result of the identification of the limit of T_f at infinite time with T_a. To introduce a different hypothesis in regard to this point, the equations of the model in refs 17 and 18 are expressed in terms of the configurational entropy of the system $S_c(t)$ instead of the fictive temperature $T_f(t)$. The model keeps the main assumptions of NM or SH models but is able to introduce different expressions for the function S_c^{lim} (see below), the configurational entropy value attained at infinite time during the structural relaxation process. We will call $S_c^{eq}(T)$ the extrapolation of the configurational entropy curve determined at temperatures above T_g to T (see Figure 2a). Several experimental data support the idea that the enthalpy (and entropy) of the limit state attained at infinite time is higher than the equilibrium value.[19−22] A possible explanation for this behavior is the collapse of the configurational rearrangements when the number of configurations available for the polymer segments attains a certain limit. When this limit is reached, the system is in a metastable state and no further decrease of the configurational entropy is possible under isothermal conditions. Thus, the equilibrium states would not be attainable with the kind of processes described in this work.

The details of this model have been given elsewhere,[17,18] and here only the main equations will be included.

The evolution of the configurational entropy in response to a thermal history that consists of a series of temperature jumps from T_{i-1} to T_i at time instants t_i, followed by isothermal stages is given by

$$S_c(t) = S_c^{lim}(T(t)) - \sum_{i=1}^{n}\left(\int_{T_{i-1}}^{T_i} \frac{\Delta c_p^{lim}(T)}{T}\,dT\right)\phi(\xi - \xi_{i-1}) \tag{1}$$

where ξ is the reduced time:

$$\xi = \int_0^t \frac{dt'}{\tau(t')} \tag{2}$$

The function $\tau(t)$ is taken according the Adam−Gibbs[23] equation extended to nonequilibrium states:

$$\tau(T,S_c) = A\exp\left(\frac{B}{TS_c(\xi,T)}\right) \tag{3}$$

and the relaxation function is assumed to be of the Kohlrausch−Williams−Watts[24] type:

$$\phi(\xi) = \exp(-\xi^{\beta}) \tag{4}$$

$S_c^{lim}(T)$ represents the value of the configurational

entropy attained in the physical aging process at infinite time and $\Delta c_p^{\lim}(T)$ is defined through

$$S_c^{\lim}(T_i) - S_c^{\lim}(T_{i-1}) = \int_{T_{i-1}}^{T_i} \frac{\Delta c_p^{\lim}(T)}{T}\, dT \qquad (5)$$

Thus, if T^* is a temperature above the glass transition region, then for any temperature T, in the glass transition temperature interval or below

$$S_c^{\lim}(T) = S_c^{eq}(T^*) + \int_{T}^{T^*} \frac{\Delta c_p^{\lim}(T)}{T}\, dT \qquad (6)$$

$$S_c^{eq}(T) = \int_{T_2}^{T} \frac{\Delta c_p(T)}{T}\, dT \qquad (7)$$

where $\Delta c_p(T)$ is the conformational heat capacity, here taken as the difference between the heat capacities of the liquid and the glass, $\Delta c_p(T) = c_{pl}(T) - c_{pg}(T)$, and T_2, the lower limit in (7), is the Gibbs−DiMarzio[25] temperature at which the configurational entropy in the equilibrium liquid would vanish.

The definition of $S_c^{\lim}$ introduces new fitting parameters in the model which, in principle is not desirable. Although a set of DSC thermograms measured on a sample submitted to a series of different enough thermal histories contains a great amount of information, it would be hardly justifiable to fit them with a model with more than four or five adjustable parameters unless it could be demonstrated that some of them can be determined independently from the results of some specific experiment. Regarding this point the very definition of the arguments of the function $S_c^{\lim}$ can be a problem. If the difference between $S_c^{\lim}$ and S_c^{eq} has a kinetic origin, then the value of $S_c^{\lim}(T_a)$ may certainly depend on the thermal history undergone by the material to attain the temperature T_a. We have no information at this stage, neither experimental nor theoretical, about such a dependence of $S_c^{\lim}$, and any hypothesis to define mathematically this function would introduce several additional parameters. Thus, at this stage, the model assumes simply that $S_c^{\lim}$ depends only on T_a. Again, there is no information on the form of the function $S_c^{\lim}(T_a)$, and thus in refs 17 and 18 it was decided to take a very simple shape in order to introduce a single additional parameter. $S_c^{\lim}(T_a)$ was defined as shown in Figure 2a. The slope of the $S_c^{\lim}(T)$ curve is smaller than the one of $S_c^{eq}(T)$ at temperatures below the glass transition. The change of slope approaching the equilibrium values is gradual, covering a temperature interval of 15 K. The failure of the extrapolated equilibrium line determined at temperatures above the glass transition to estimate the limit states of the structural relaxation process has been found very close to the glass transition temperature interval;[19−22] thus the change of slope shown in the sketch of Figure 2a, determined by the reference temperature T_{ref}, should be quite coincident with the glass transition temperature interval. We assume in the calculations a value for T_{ref} equal to the glass transition temperature determined as the intersection point of the glass and liquid enthalpy lines, as determined from the scan measured after cooling the sample at 40 K min^{-1} from a temperature above the glass transition. Only the model simulation of the scans measured after annealing at temperatures very close to T_{ref} is expected to be significantly dependent on the details of the form of $S_c^{\lim}(T_a)$, or on the value accepted for T_{ref}. For instance, very small differences in the quality of the model fit or in the values of the model parameters are found when this temperature is changed within 3 K, the interval of variability of the glass transition usually found for a change in the cooling rate within the experimental possibilities of the technique.

This assumption introduces a single additional parameter in the model but, as pointed out in ref 18, it renders the origin of the difference between $S_c^{\lim}(T)$ and $S_c^{eq}(T)$ as a kinetic effect of the nonequilibrium relaxation process, indistinguishable from an eventual curvature of the equilibrium entropy line around the glass transition, an argument advanced with the aim of resolving the Kauzmann paradox,[26] a feature also suggested from the temperature dependence of equilibrium specific volume.[27]

Thus, the model equations contain five adjustable parameters: δ and T_2 in the definition of the $S_c^{\lim}(T)$ function, A and B in eq 3, and β to characterize the form of the relaxation function.

It has been shown, and the results in this work also support this idea, that the agreement between the model simulation and the experiments is highly improved with the model proposed in refs 17 and 18 with respect to the NM or SH predictions.[17,18,28−30]

Experimental Section

The polystyrene sample was a Polysciences standard with a number average molecular weight of 37 000. Poly(4-hydroxystyrene) was obtained from Polysciences.

Samples of poly(4-methylstyrene) (P4MS) and poly(4-chlorostyrene) were synthesized following an identical procedure. Monomers, purchased from Aldrich, were washed twice with a 10% NaOH solution and then with deionized water until a neutral pH was obtained. The monomers were then dried with $CaCl_2$ and distilled under vacuum. Free radical polymerization was carried out under nitrogen in a 50% wt/v toluene solution with 0.1% wt/v α,α′-azobis(isobutyronitrile) (AIBN) as initiator at 333 K. The initiator concentration was chosen in order to achieve a molecular weight around 30 000.

The differential scanning calorimetry experiments were performed in a Perkin-Elmer DSC-2 calorimeter. Only a single sample of each polymer was used in this work. The sample weights were selected between 8 and 14 mg. All the DSC experiments were started by keeping the sample at $T_g + 50$ K for 10 min to ensure that it was in equilibrium. The sample was then cooled to the selected aging temperature, T_a, at 40 K min^{-1} and kept at T_a for t_a min. After this isothermal stage the sample was cooled down again at 40 K min^{-1} to the temperature selected for the start of the heating scan, $T_g - 60$ K. The heating scan took place between $T_g - 60$ K and $T_g + 50$ K at 20 K min^{-1}. Data points were collected by computer only on heating at 0.5 K intervals between $T_g - 50$ K and $T_g + 50$ K. The heat capacity of the sample was calculated from these data as previously described.[22] The cooling rate selected was the highest possible rate at which the temperature of the sample is under control throughout the whole cooling scan. All thermal treatments were carried out in the calorimeter. The $c_p(T)$ curve measured during the heating scan after cooling the sample from $T_g + 50$ to $T_g - 60$ K will be called here a reference scan.

Very reproducible DSC thermograms were obtained in all the scans measured on any sample. Some scattering was found in the absolute values of the heat capacity in the case of PS, what has to be attributed to baseline shifts of the calorimeter or to different positions of the sample pan into the DSC sample holder. This fact produces a small shift (less than 4%) in the vertical axis without change in shape and is not important for the analysis made in this work.

Results and Discussion

(i) Experimental c_p Data. The heat capacity curves of the four polymers were measured after thermal

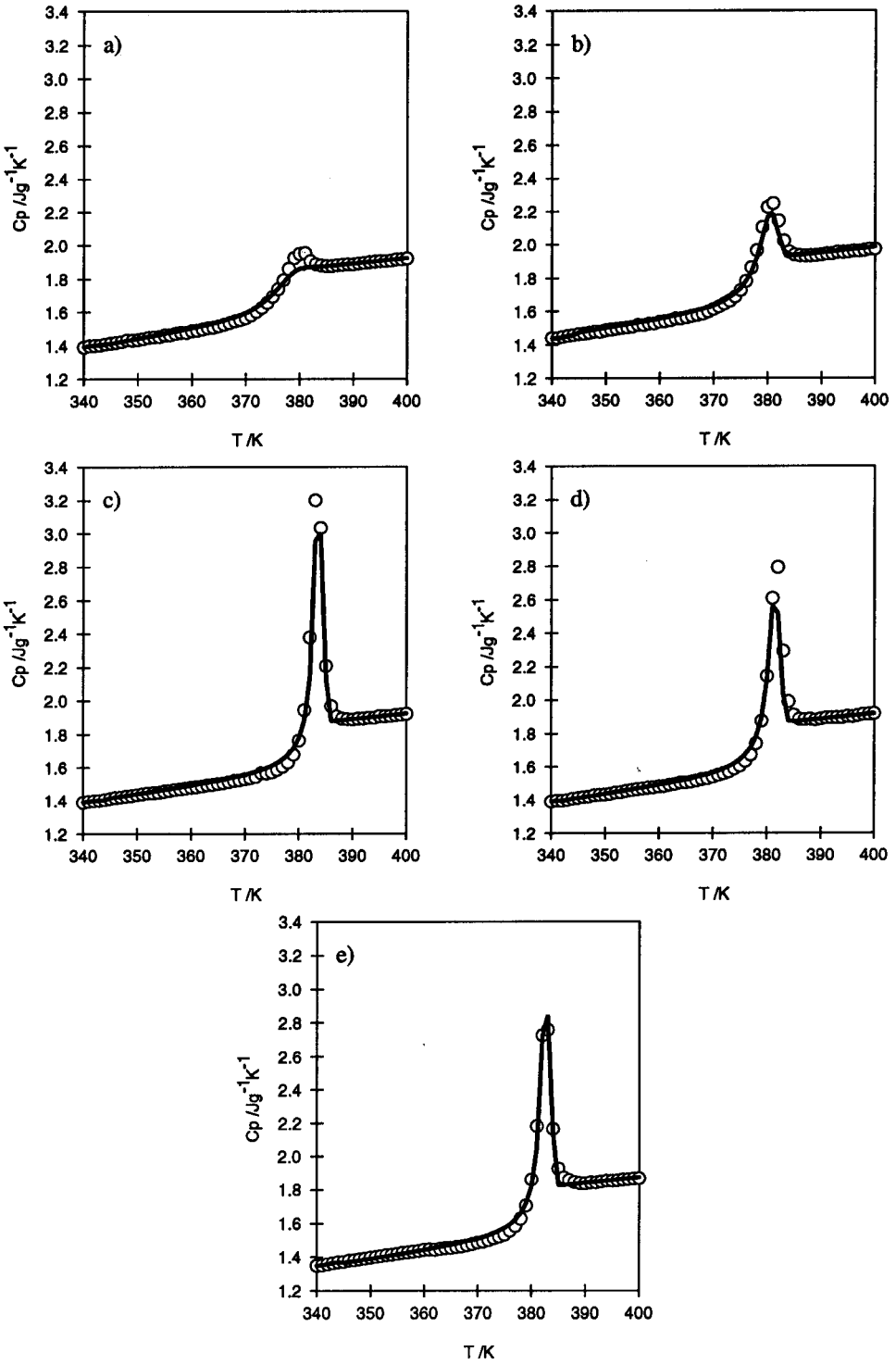

Figure 3. Temperature dependence of the heat capacity of PS measured after different thermal treatments (open circles): (a) reference scan; (b) $T_a = 368$ K, $t_a = 1000$ min; (c) $T_a = 353$ K, $t_a = 1000$ min; (d) $T_a = 353$ K, $t_a = 300$ min; (e) $T_a = 348$ K, $t_a = 1000$ min. The full line represents the calculated model curves with $B = 1000$ J g^{-1} and the other four model parameters according to Table 2.

treatments including isothermal aging at different temperatures T_a ranging between $T_g - 5$ and $T_g - 25$ in 5 K steps. The values of the aging times were between 5 and 5000 min. *In Figures 3−6* five representative sets of $c_p(T)$ data for each polymer are shown together with the predicted model curves (solid lines). One data set is the reference scan, and the others correspond to different aging times and temperatures (see the figure captions). All of the $c_p(T)$ curves measured after aging show a peak at a temperature higher than T_g. The temperature of the maximum of $c_p(T)$ depends on the aging time and temperature, as shown in Figure 7. At the lowest aging temperature (around 25 K below T_g) in PS, PMS, and PClS the peak at the shorter aging times shifts toward lower temperatures. As the aging time increases, the temperature of the peak maximum goes through a minimum around $t_a = 100$ min and then increases. The temperature of the peak maximum increases with aging time for the rest of the aging temperatures in a sigmoidal fashion. Constant values are attained at very short times when $T_a = T_g - 5$ K but they are not reached at any other aging temperature. The behavior of PHS is quite different and will be discussed below.

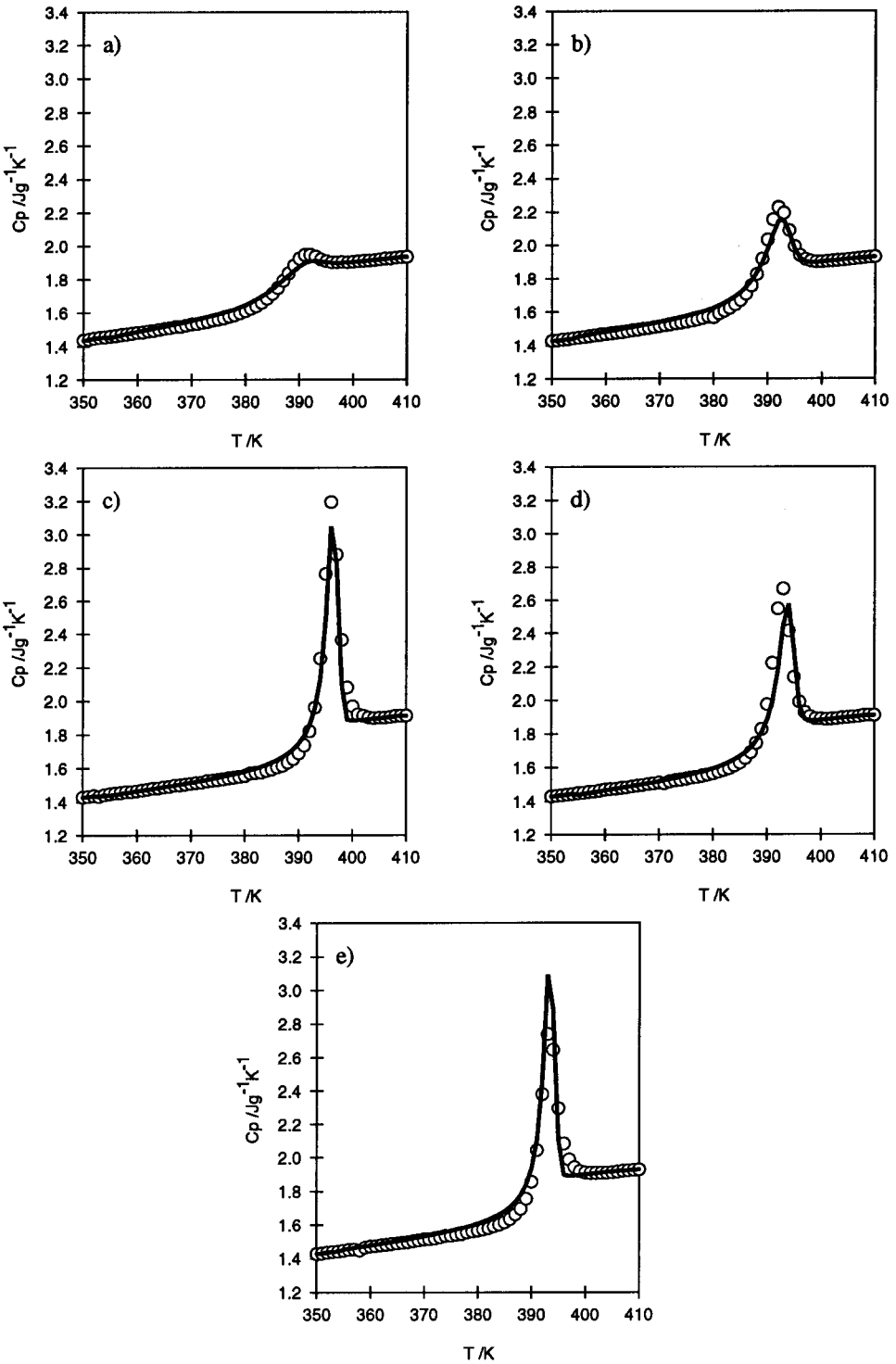

Figure 4. Temperature dependence of the heat capacity of PMS measured after different thermal treatments (open circles): (a) reference scan; (b) $T_a = 376$ K, $t_a = 800$ min; (c) $T_a = 366$ K, $t_a = 2540$ min; (d) $T_a = 366$ K, $t_a = 300$ min; (e) $T_a = 356$ K, $t_a = 1000$ min. The full line represents the calculated model curves with $B = 1000$ J g^{-1} and the other four model parameters according to Table 3.

The heat capacity of each polymer in the liquid state, $c_{pl}(T)$, was calculated by a least squares fit to a straight line of the experimental $c_p(T)$ data in the temperature interval between $T_g + 20$ and $T_g + 50$. The heat capacity in the glassy state, $c_{pg}(T)$, was also fitted to a straight line in the temperature interval between $T_g - 50$ and $T_g - 20$ K. The conformational heat capacity is considered to be the difference $\Delta c_p = c_{pl} - c_{pg}$, and, as a consequence, it also has a linear dependence with temperature. The $\Delta c_p(T)$ equations obtained by least squares analysis for the four polymers are listed in Table 1. The glass transition temperature was determined in each polymer as the point of the intersection of the enthalpy lines in the liquid and glassy states, calculated from the reference scan (see Figure 1). This temperature has been called the fictive temperature in the glassy state T_f' and can be calculated by the integration of the $c_p(T)$ curve.[31] The T_g and $\Delta c_p(T_g)$ data for the four polymers are also shown in Table 1.

Small differences (9 K) in the glass transition temperature are reported in Table 1 for PMS with respect to PS. This modest change may be mainly due to a small increase in the molar volume of the side group with the methyl group providing slightly more steric

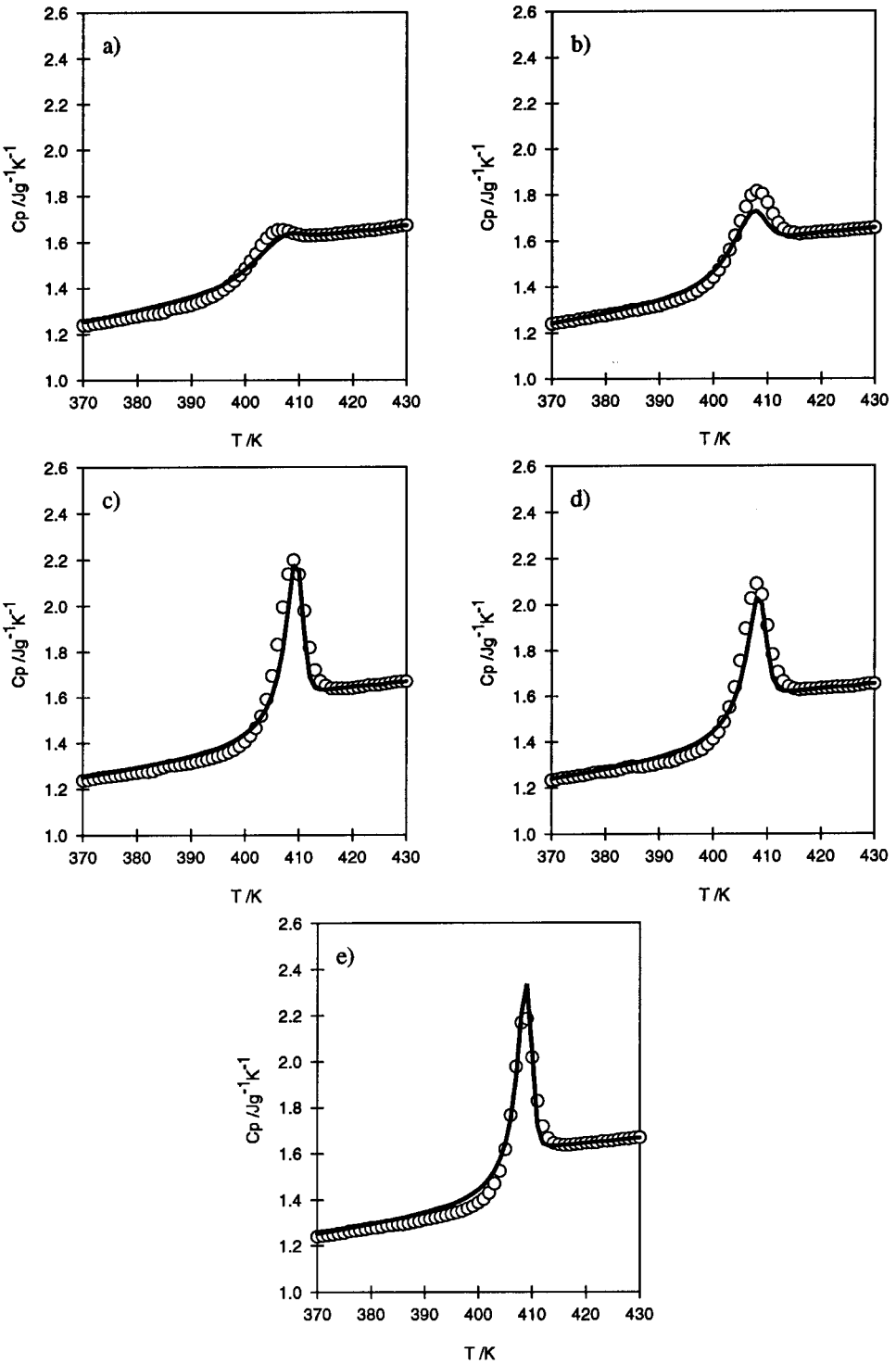

Figure 5. Temperature dependence of the heat capacity of PClS measured after different thermal treatments (open circles): (a) reference scan; (b) $T_a = 395$ K, $t_a = 600$ min; (c) $T_a = 383$ K, $t_a = 1000$ min; (d) $T_a = 383$ K, $t_a = 300$ min; (e) $T_a = 373$ K, $t_a = 800$ min. The full line represents the model calculated curves with $B = 1000$ J g^{-1} and the other four model parameters according to Table 4.

hindrance than hydrogen. The glass transition temperature of PClS is higher than that of PMS and a broadening of the glass transition is reflected in an increase of the parameter ΔT. This may be explained by taking into account the need for more energy to give free mobility to the dipoles. The presence of the hydroxyl groups generated the most profound changes in the physical properties of the polymer. The T_g of PHS is in the temperature range of poly(α-methylstyrene), and the value of ΔT is still larger than in the other polymers of the series. Although it is possible that such a high T_g is due to an increase in main chain stiffness, it is believed that intra- and intermolecular interactions, which lead to an even further decrease in free volume, are the main cause. As the width of the glass transition, ΔT (see Table 1) increases in the sequence PS−PMS−PClS−PHS, so too the peaks appearing in the $c_p(T)$ curves measured after aging broaden in the same order (see Figures 3−6). In the case of PHS, the broadening of the glass transition region is even more apparent in the dependence of the temperature of the peak in the $c_p(T)$ curves with the aging temperature. While in PS, PMS, and PClS, the temperature of the $c_p(T)$ maxima is within a narrow temperature interval of approxi-

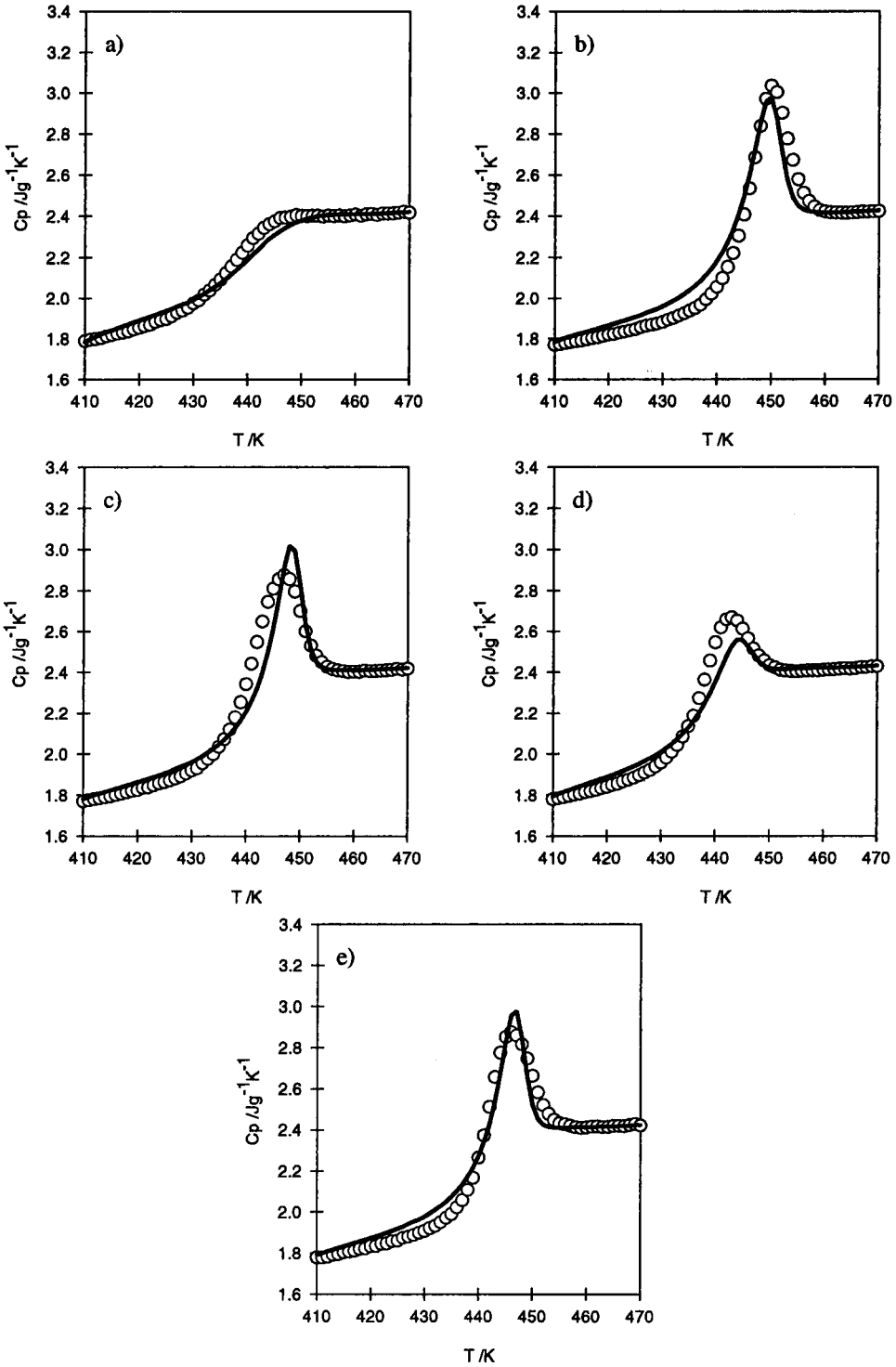

Figure 6. Temperature dependence of the heat capacity of PHS measured after different thermal treatments (open circles): (a) reference scan; (b) $T_a = 423$ K, $t_a = 1000$ min; (c) $T_a = 418$ K, $t_a = 1000$ min; (d) $T_a = 418$ K, $t_a = 100$ min; (e) $T_a = 413$ K, $t_a = 1000$ min. The full line represents the model calculated curves with $B = 1000$ J g^{-1} and the other four model parameters according to Table 5.

Table 1. Characteristic Parameters of the Glass Transition for the Four Polymers PS, PMS, PClS, and PHS

	PS	PMS	PClS	PHS
T_g (K)	373	382	398	433
ΔT (K)	4.7	6.3	7.4	14.1
$\Delta c_p(T)$ (J g^{-1} K^{-1})	$(0.782-1.34) \times 10^{-3}T$	$(0.710-1.17) \times 10^{-3}T$	$(0.614-0.89) \times 10^{-3}T$	$(1.879-3.23) \times 10^{-3}T$
$\Delta c_p(T_g)$ (J g^{-1} K^{-1})	0.28	0.26	0.26	0.48
$T_g\Delta c_p(T_g)$ (J g^{-1})	105.2	100.85	103.5	208.3

mately 6 K, centered around $T_g + 9$ K for any aging temperature, in PHS the peaks appear from T_g up to $T_g + 17$ K depending on the aging temperature.

(ii) Results of Modeling Studies. The modeling was carried out by replacing the cooling and heating stages by a series of 1 deg temperature jumps followed

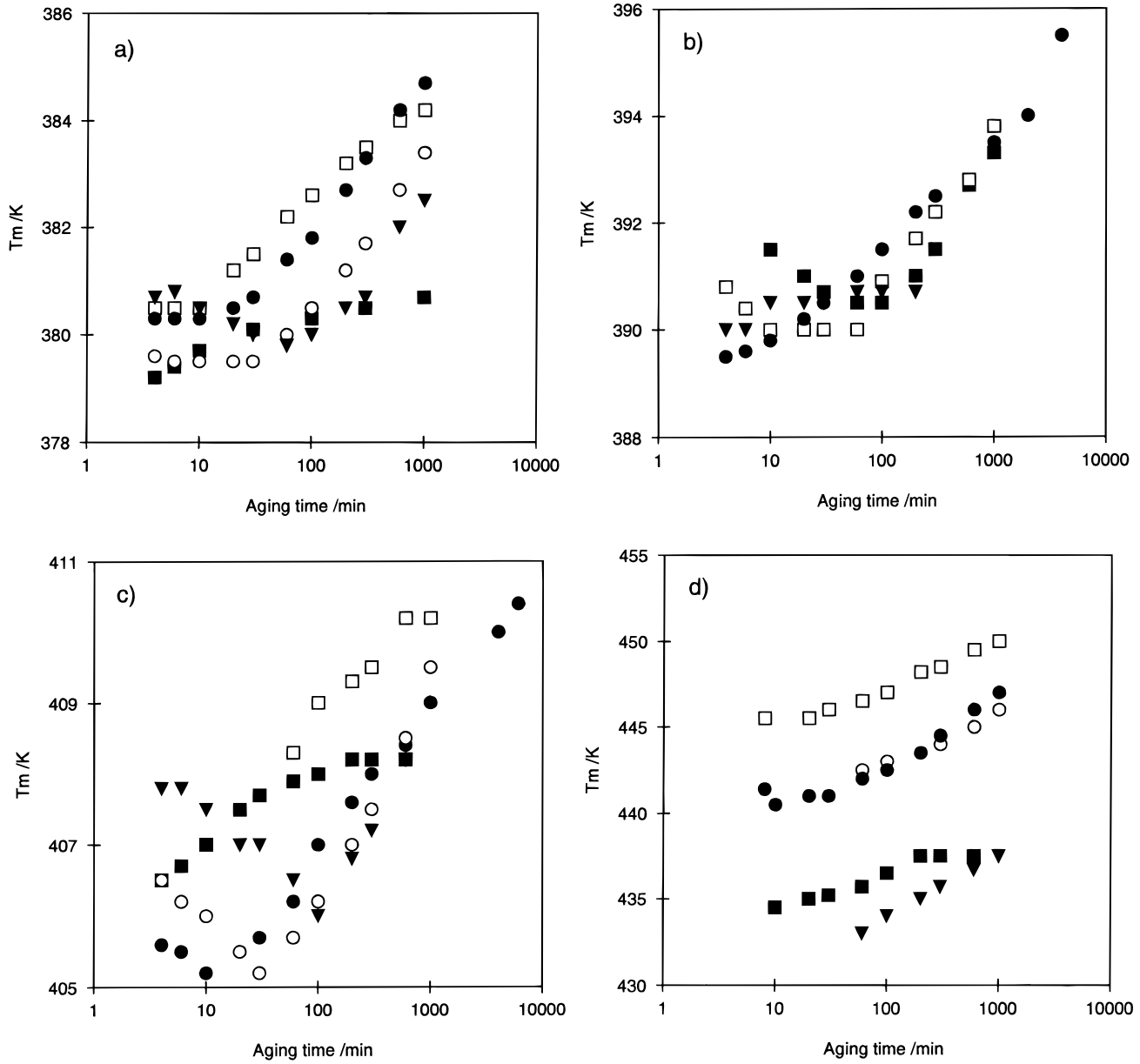

Figure 7. Temperature of the maxima shown by the $c_p(T)$ curves as a function of the aging time for different aging temperatures. (a) PS; (b) PMS; (c) PClS; (d) PHS. In (a), (c), and (d): (■) $T_a = T_g - 5$ K; (□) $T_a = T_g - 10$ K; (●) $T_a = T_g - 15$ K; (○) $T_a = T_g - 20$ K; (▼) $T_a = T_g - 25$ K. In (b): (■) $T_a = T_g - 6$ K; (□) $T_a = T_g - 11$ K; (○) $T_a = T_g - 21$ K; (▼) $T_a = T_g - 26$ K.

by isothermal stages with a duration fixed to lead to the same overall rate of temperature change as in the experiments. The configurational entropy was calculated at time intervals t_k by means of eq 1, and the relaxation time at this instant is then calculated using eq 3. This value of the relaxation time is used to calculate the reduced time at the subsequent time instant t_{k+1}, according to eq 2. After each temperature jump the reduced time was evaluated at time intervals $t_k = 0.01 \times 2^k$ s with integer k. Reference 17 gives more details of the algorithm used to obtain the predicted values of c_p.

The parameters of the model are supposed to be material parameters, independent of the thermal history. The model, with a single set of parameters should be able to reproduce the $c_p(T)$ curves measured after any thermal history. Thus, the set of parameters of each polymer was determined by simultaneous least squares fit to a series of $c_p(T)$ experimental curves measured after thermal histories covering a broad range of aging temperatures and times. The sets of experimental curves included in Figures 3−6 were considered representative enough of the behavior of each material in relation to the structural relaxation process. It was checked that the parameters determined from sets of experimental curves different from those shown in the figures were not significantly different in any of the polymers from the ones presented here.

The correlation between the parameters of the model has been reported in other polymers.[17,18,28−30] The problem is similar to what happens in the other phenomenological models such as those of Narayanaswamy−Moynihan or Scherer−Hodge.[2,3,8,14,22,32−34] Mainly a correlation is found between B, A, and T_2. To avoid this problem, the parameter B was fixed while the others were determined with the least squares routine. The fitting procedure was conducted with different values of B. The Nedler and Mead[35] search routine was employed.

The model with the assumptions of $S_c^{lim}(T) = S_c^{eq}(T)$ leads to quite poor fits of the experimental data with this assumption, and for any value of B it is impossible

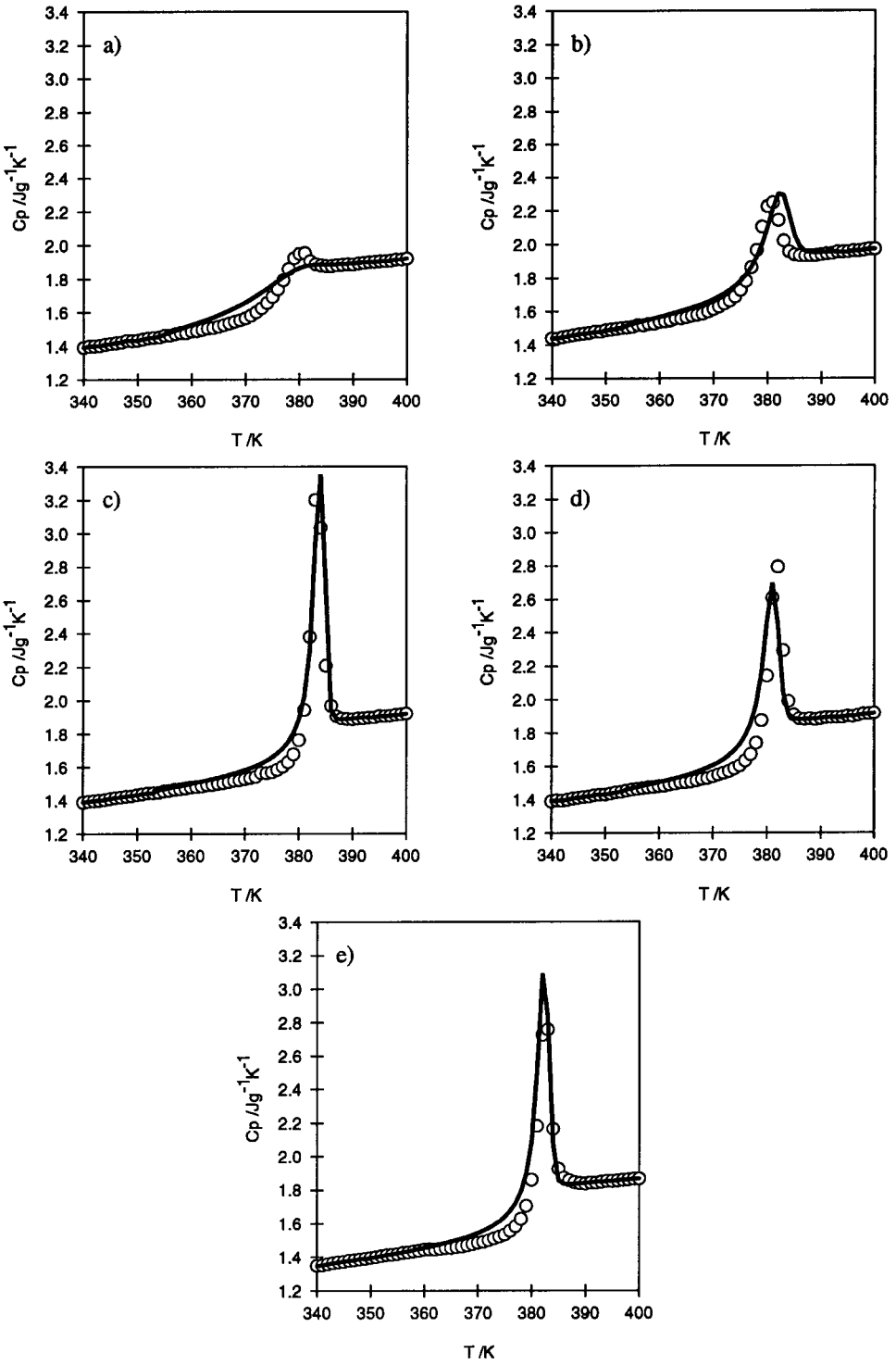

Figure 8. Best model simulation of the five experimental $c_p(T)$ curves of PS, under the assumption of $S_c^{lim}(T) = S_c^{eq}(T)$. The value of $B = 1000$ J g^{-1} was fixed in the simultaneous least squares search routine of the five experimental $c_p(T)$ curves. The set of parameters found was $\beta = 0.38$, $T_2 = 304.3$ K, and ln $A = -35.6$ (s).

Table 2. Set of Model Parameters Found by the Search Routine for PS with Different Values of *B*

B/J g^{-1}	δ/J g^{-1} K^{-1}	β	T_2/K	ln A (s)
500	0.151	0.40	333	−32.3
1000	0.157	0.46	315	−43.4
1500	0.159	0.51	301	−50.6
2000	0.159	0.56	289	−55.9
2500	0.159	0.60	278	−60.1
3000	0.158	0.63	269	−63.6

Table 3. Set of Model Parameters Found by the Search Routine for PMS with Different Values of *B*

B/J g^{-1}	δ/J g^{-1} K^{-1}	β	T_2/K	ln A (s)
500	0.12	0.41	331	−26.9
1000	0.12	0.46	309	−35.7
1500	0.11	0.50	291	−41.2
2000	0.11	0.53	277	−45.1
2500	0.11	0.56	262	−48.4
3000	0.11	0.59	252	−50.5

to reproduce simultaneously the experimental results obtained after aging at high and low aging temperatures. As an example, Figure 8 shows the model simulation under this assumption, with $B = 1000$ J g^{-1} for PS (the set of parameters found in the least squares search routine are given in the figure caption). The

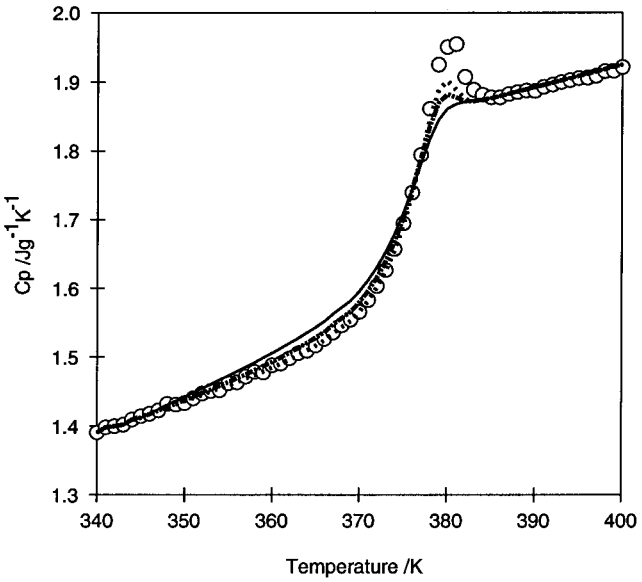

Figure 9. Model simulation of the reference scan of PS with $B = 1000$ J g^{-1} (—), $B = 2000$ J g^{-1} (—···—), and $B = 3000$ J g^{-1} (···) and the rest of the parameters according to Table 2. The curves calculated for the other four thermal histories of Figure 4 with the different values of B are nearly superimposable and are not shown. The open circles represent the experimental data.

Table 4. Set of Model Parameters Found by the Search Routine for PClS with Different Values of Parameter *B*

B/J g^{-1}	δ/J g^{-1} K^{-1}	β	T_2/K	ln A (s)
500	0.120	0.38	345	−27.9
1000	0.118	0.42	322	−37.5
1500	0.116	0.46	305	−43.9
2000	0.115	0.49	290	−48.7
2500	0.115	0.52	278	−52.7
3000	0.113	0.54	267	−55.6

Table 5. Set of Model Parameters Found by the Search Routine for PHS with Different Values of Parameter *B*

B/J g^{-1}	δ/J g^{-1} K^{-1}	β	T_2/K	ln A (s)
1000	0.178	0.28	382	−25.9
2000	0.171	0.30	362	−36.1
3000	0.160	0.31	347	−43.5
4000	0.153	0.32	334	−48.6
5000	0.149	0.33	323	−53.0
6000	0.140	0.34	314	−56.8
7000	0.137	0.35	306	−60.1
8000	0.135	0.36	297	−62.5

same behavior is also shown by the other polymers. However, when in the model equations $S_c^{lim}(T)$ is as represented in Figure 2a by the dashed lines, the agreement between experiment and model calculations is very good (taking into account that a single set of parameters is used to reproduce the $c_p(T)$ curves measured after different thermal histories) in PS, PMS, and PClS, as shown in Figures 4−6. The discrepancies are greater in the case of PHS but the fit is still clearly acceptable (Figure 7). The definition of the shape of $S_c^{lim}(T)$ introduces a new parameter in the model, δ. Thus, with each value of the parameter B fixed, the search routine found a set of four parameters, δ, β, T_2, and A, that except for δ were systematically dependent on the value of B (Tables 2−5). Nevertheless, the model simulation for any thermal history, with the different sets of parameters, shown in the tables, yields nearly the same $c_p(T)$ curve, the only exception in the case of the polymers in this work is the reference scan in which it is possible to detect a slight systematic dependence of the shape of the $c_p(T)$ curve with the value of B, in fact the accuracy of the fit increases with the value of B. As an example, three model calculations of the reference scan of PS with different values of B (and the rest of parameters according to Table 2) are represented in Figure 9.

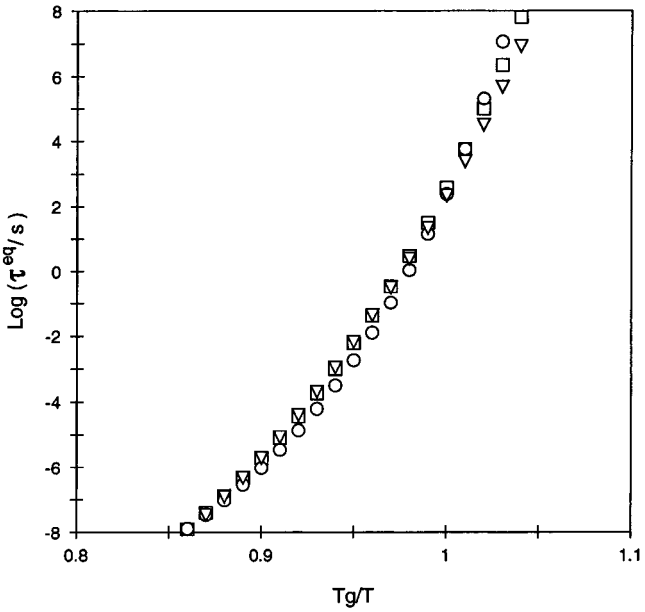

Figure 10. Temperature dependence of the equilibrium relaxation times, $\tau^{eq}(T)$, calculated for PS with $B = 1000$ J g^{-1} (○), $B = 2000$ J g^{-1} (□), and $B = 3000$ J g^{-1} (▽) and the rest of the parameters according to Table 2.

The analysis of the numerical values of the model parameters needs, first of all, some further information to help determine the value of one of the parameters independently from the rest, and thus decide which set of model parameters is the physically acceptable, or at least to diminish the interval of uncertainty. It should be noted that some information contained in Tables 2−5 can be analyzed without this kind of consideration.

The value of the δ parameter in PS, PMS, and PClS is nearly independent of the value of B fixed in the least squares routine. It corresponds to 53% of the $\Delta c_p(T_g)$ in the case of PS and around 45% in PMS and PClS. That means that the limit states of the structural relaxation process are quite far from the extrapolated equilibrium line. In the case of PHS this parameter is around 35% of the $\Delta c_p(T_g)$, but it depends slightly on the value of B, probably because the fit in this polymer is not as accurate as in the other polymers. As the error in the fit increases, the uncertainty in the determination of the model parameters is higher, as different sets of parameters can yield model curves with a similar value of the error function.

The temperature dependence of the relaxation times (to simplify we call relaxation time the parameter τ in eq 2) in equilibrium conditions can be calculated from the values of the parameters B, T_2, and A:

$$\tau^{eq}(T) = A \exp\left(\frac{B}{TS_c^{eq}(T)}\right) \qquad (8)$$

As has been reported in other polymers, the different sets of parameters found in the search routine for the different values of B yield nearly the same $\tau^{eq}(T)$, as shown, as an example, in Figure 10 for PS. This is probably the reason for the correlation between the values of B, T_2, and A in the model. The different sets of parameters predict very similar values of the relax-

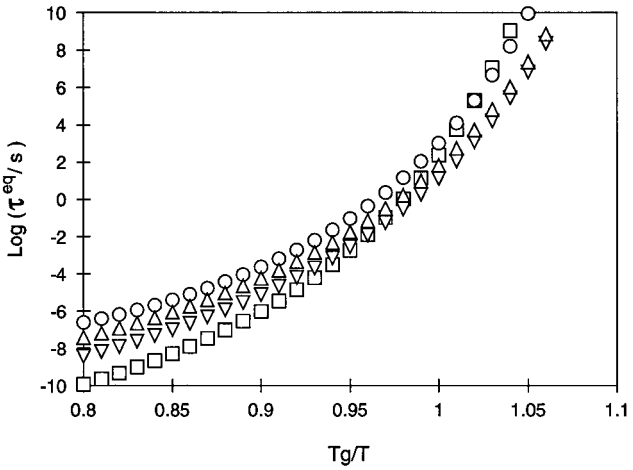

Figure 11. Temperature dependence of the equilibrium relaxation times, $\tau^{eq}(T)$, calculated for PS with $B = 1000$ J g^{-1} (□), PMS with $B = 1000$ J g^{-1} (△), PClS with $B = 1000$ J g^{-1} (▽), and PHS with $B = 2000$ J g^{-1} (○).

ation time in equilibrium and probably the same happens in out of equilibrium states, during the structural relaxation process. As a consequence, the same $c_p(T)$ curves are predicted. As the value of B increases, the curvature of $\tau^{eq}(T)$ slightly diminishes and the vertical asymptote shifts toward lower temperatures, so that the difference $T_g - T_2$ increases.

The $\tau^{eq}(T)$ curve can itself be considered a material parameter, determined uniquely from the $c_p(T)$ curves measured after different thermal histories. Figure 11 represents these "calorimetric" structural relaxation times curves for the four polymers of the series. At temperatures above T_g the slope of $\tau^{eq}(T)$ decreases with any of the para substituents of the PS monomeric unit. The behavior of PMS and PClS is still coincident at temperatures lower than T_g but in this temperature interval the slope of the $\tau^{eq}(T)$ curve of PHS is higher.

The change of slope is enough to take account in the model simulation for the enlargement of the peaks appearing in the $c_p(T)$ curves after aging. In the case of polymers and thermal histories in which no sub-T_g peaks appear (as is the case of the experiments in this work) during the heating scan, after aging, the mobility of the polymer main chain segments is very small at low temperatures, the relaxation times are several orders of magnitude above the experimental times at the start of the measuring scan, and consequently, as the temperature rises, the enthalpy of the material evolves according to the glassy behavior. The relaxation time increases with temperature during the scan but it only arrives at values on the order of magnitude of the experimental times when the temperature attains a value (of course dependent of the thermal history) higher than the onset of the glass transition and usually above T_g. As the temperature still increases, the experimental dependence of the relaxation times with temperature causes the quick approach of the enthalpy to its equilibrium values, producing the peak in $c_p(T)$. The more or less pronounced dependence of the relaxation time with temperature in this temperature interval above T_g highly influences the rate of approach of the enthalpy to equilibrium and consequently affects the shape of the $c_p(T)$ curve. Clearly, many other parameters influence the shape of the measured $c_p(T)$; as the relaxation time that controls the rate of the structural relaxation process is the out-of-equilibrium one that depends at any temperature also on the previous thermal history and on the β parameter too. Nevertheless it has been shown in the series of methacrylate polymers[28] that only a change in the slope of $\tau^{eq}(T)$ is enough to explain the broadening of the transition region as the side group becomes larger, nearly without change of the β parameter, i.e. in the width of the distribution of relaxation times. PMS and PClS are also two examples of this behavior, but as we will show below the case of PHS is different also in this aspect.

The curvature of the $\tau^{eq}(T)$ plot can be analyzed in terms of the fragility parameter, D, defined by Angell from the temperature dependence of the viscosity[36]

$$\eta = \eta_0 \exp\left(\frac{DT_0}{T - T_0}\right) \tag{9}$$

Fragile materials, the class in which polymers can be included, are characterized by high values of $\Delta c_p(T_g)$, low values of D (not higher than 13 for polymers, the value found for the most fragile materials is 3.2), and the ratio T_g/T_0 (between 1.1 and 1.3). On the contrary strong materials present high values of D (even above 30) and T_g/T_0 (up to 1.9).

An approximate relationship between the parameters of eqs 3 and 9 is useful to compare calorimetric and viscosity data. A very simple equation can be deduced if one identifies T_0 with T_2, and if the temperature dependence of the conformational heat capacity can be expressed as

$$\Delta c_p(T) = \frac{T_g \Delta c_p(T_g)}{T} \tag{10}$$

then one finds that

$$\tau^{eq}(T) = A \exp\left(\frac{B}{T_g \Delta c_p(T_g)} \frac{T_2}{T - T_2}\right) \tag{11}$$

Although eq 11 is different from the linear expression we have taken for $\Delta c_p(T)$ and the preexponential factor A in eq 3 is in this work an adjustable parameter, the approximation

$$D = \frac{B}{T_g \Delta c_p(T_g)} \tag{12}$$

obtained by comparison of eqs 12 and 10 can be enough for the purposes of this discussion.

In the same way that a $\tau^{eq}(T)$ curve is compatible, within the accuracy of the model, with a broad range of values of B in eq 6, it is also compatible with a broad range of values of D. The different slope of $\tau^{eq}(T)$ between PS and the polystyrene derivatives seems to be representative of a less fragile behavior of the latter ones; nevertheless no great differences in the value of D are expected between PS, PMS, and PClS, because of their molecular similarities. In fact the interval of variation of D in amorphous polymers should not be great.

We take as reference to compare the model parameters in the four polymers $B = 1000$ J g^{-1}; thus the value of T_2 for PS is 315 K, very close to the value reported for T_0 from viscosity measurements by Adam and Gibbs[23] ($T_0 = 311$ K) and by Miller[37] ($T_0 = 323$ K). With this value of B, the value of D for the three polymers would be around 10, as shown in Table 6. The case of PHS could be different. Although, in fact, the shape of the $\tau^{eq}(T)$ plot is very similar to that of PMS and PClS,

Table 6. Comparison between the Model Parameters of the Four Polymers

	PS	PMS	PClS	PHS
B/J g^{-1}	1000	1000	1000	2000
D	9.5	9.9	9.7	9.6
T_2/K	314.6	308.8	321.8	361.6
$T_2 - T_g$/K	58.4	73.2	76.2	71.4
T_g/T_2	1.19	1.24	1.24	1.20
β	0.46	0.46	0.42	0.30
ln A	−43.4	−37.5	−35.7	−36.1
A	1.4×10^{-19}	5.2×10^{-17}	3.2×10^{-16}	2.1×10^{-16}
δ/J g^{-1} K^{-1}	0.16	0.11	0.12	0.17

the hydrogen bonding interaction between chain segments might play a significant role in this aspect. Low molecular weight alcohols form a special class of materials in regard to their glass transition behavior. They present high values of $\Delta c_p(T_g)$ but still more divergent behavior reflected by the shape of the temperature dependence of the viscosity,[36] and also higher values of the D parameter than similar materials with no hydrogen bonding interaction. The conformational heat capacity of PHS is about twice that of the other polymers in the series; $T_g\Delta c_p(T_g)$ is also approximately twice the value of this parameter in PS, PMS, and PClS. That means that the same value of D in the four polymers would mean a value of $B = 2000$ J g^{-1} in PHS, but by analogy to what happens in low molecular weight alcohols, higher values of B can also be considered perhaps up to twice this value, i.e. 4000 J g^{-1}.

Thus, Table 6 presents the model parameters found for PS, PMS, and PClS with $B = 1000$ J g^{-1} and PHS with $B = 2000$ J g^{-1}.

To a certain extent, the values of the model parameters calculated in this work can be compared with their counterparts in other phenomenological models. Many studies on the structural relaxation of PS by means of calorimetric methods can be found in the literature.[6,14,38−41] Several series of DSC thermograms measured after different thermal histories have been fitted to the NM or SH models. On the contrary there are no precedent studies of this type on PMS, PClS, and PHS.

The set of model parameters determined with the NM model by curve fitting to individual thermograms have been found to be strongly dependent of the thermal history; for instance, although mean values are given in ref 2 for the parameter β of the KWW equation in the SH model, $\beta = 0.6 \pm 0.08$, values of this parameter ranging between 0.5 and 1 can be found in refs 41 and 42 for different thermal histories conducted on a single sample of PS. Something similar was found in ref 14. It seems that the dependence of the model parameters with the thermal history, that has been found in many materials, is especially important in this polymer, and this can explain the great differences found by different authors fitting analogous DSC results. Thus, Hodge and Huvard[6] calculated a value for β of 0.68 with their experimental results but $\beta = 0.39$ by curve fitting to the data of Chen and Wang,[39] Privalko et al.[40] report that β slightly depends on the molecular weight in monodisperse polystyrenes, with a value around 0.5; Hutchinson[43] found a value of $\beta = 0.47$. With the SH model a value of $\beta = 0.74$ has been reported.[14]

It has been pointed out that the value of β found by means of curve fitting with the SH model[2,33] or with the model used in this work[17,18,28−30] is in many polymers close to the value determined with dielectric or dynamic-mechanical spectroscopies. The value for β we determine in this work for the curve fitting with $B = 1000$ J g^{-1} is close to the dielectric one, thus the results of Saito and Nakajima[44] allows one to estimate a value for β around 0.35, a similar value, 0.4, is accepted by Hodge for the dielectric relaxation.[34] The dynamic-mechanical relaxation spectra measured on monodispersed PS of different molecular weights[45] allows one to estimate a higher value of the β parameter, between 0.6 and 0.65 depending on the molecular weight of the sample.

Although the value of T_2 depends on the value of B, and in the case of PS the agreement with the viscosity results has been used as a reference to select a set of parameters from Table 2, it is noteworthy that for any value of B, T_2 is in the interval between T_0 and the Kauzmann temperature, 281 ± 15 K determined by Karasz et al.[46] (in this reference it is reported that $T_g - T_0 = 82 \pm 15$ K; the PS sample had a glass transition temperature of 362 K) and 261 K by Abu-Isa and Dole[47] and Miller.[48] On the contrary the SH model leads to a value of 210 K,[14] much lower than any of these.

The temperature dependence of the relaxation times in the glass transition temperature can be used to define an effective activation energy through

$$\frac{\partial \ln \tau^{eq}}{\partial(1/T)} = \frac{\Delta h^*}{R} \tag{13}$$

in coincidence with the equation used in the NM model for the relaxation time when applied to equilibrium states.[3] This effective activation enthalpy can in turn be calculated from the dependence of the glass transition temperature on the cooling rate from an equilibrium state above the glass transition.

$$\frac{\partial \ln q_c}{\partial(1/T_g)} = \frac{\Delta h^*}{R} \tag{14}$$

The values reported for $\Delta h^*/R$, calculated from eq 14 range between 70 and 130 kK (see ref 2 and the references cited therein). It is possible to use eq 13 to determine $\Delta h^*/R$ from the values of B, T_2, and ln A. We obtain $\Delta h^*/R = 102$ kK from our curve fitting with $B = 1000$ J g^{-1}, this value is higher than the average value given in ref 2 but in good agreement with the one calculated by Privalko et al.[40] for a PS with a molecular weight close to that of our sample.

The most interesting point is that the β parameter takes the same value in PS, PMS, and PClS, around 0.45, but the value for PHS is somewhat smaller at 0.3, and even if the value of B were much higher than 2000 J g^{-1}, the conclusion would not change because, as shown in Table 5, the value of β is below 0.35 up to $B = 7000$ J g^{-1}. This means that the distribution of relaxation times in PHS is much broader than in the rest of the polymers of the series, which is not an unexpected fact due to the presence of intra- and interchain molecular connectivity caused by hydrogen bonding. The overlapping of the breakage and re-formation of hydrogen bonds with the conformational rearrangements may produce an overall relaxation process characterized by a relaxation function more complicated than that described by the KWW equation. This can explain the difficulties of the model to reproduce the experimental $c_p(T)$ curves in this polymer. With these values of B, the parameters T_2 and the pre-exponential factor A also take very reasonable values. T_g/T_2 is around 1.20 in PS and PHS and slightly higher, 1.24, in PMS and PClS due to the smaller slope of $\tau^{eq}(T)$ but always within what

is expected for amorphous polymers. The difference $T_g - T_2$ is also within the values found in the viscoelastic main relaxation.[23,30]

Concluding Remarks

The structural relaxation of styrenic polymers below T_g is marginally influenced by the substituents in the para position. The hydroxyl group is the only exception to this general observation because of the influence of hydrogen bonding. The Gómez−Monleón model was used in this work to fit experimental C_p data and to describe these materials in terms of theoretical parameters. It showed good fitting capability for a wide range of thermodynamic and kinetic conditions below T_g. In addition, reliable results achieved with different polymers support the view that the theoretical foundations of this model are essentially correct. The characteristic parameters required to describe the physical aging of a material were also in agreement with expectations. Although a wider range of cases has to be studied, the Gómez−Monleón model certainly appears to offer an improvement in the understanding of the phenomena governing sub-T_g structural relaxation. In more general terms, the results presented here indicate that polymeric relaxation is not influenced by the nature of a rigid side group, i.e., an aromatic ring, unless it introduces strong specific interactions. This implies that the distribution of relaxation times does not depend on steric hindrance but on flexibility. Further work is needed on the influence of the flexibility of both the main chain and side groups, in other polymeric materials.

Acknowledgment. The work of the group of the Universidad Politecnica de Valencia was partially supported by CICYT through the project MAT94-0596. J.L.G.R. wishes to thank the Spanish DGICYT and the Royal Society of London for a grant to visit Heriot-Watt University during the final stages of this work. A.B. also thanks Heriot−Watt University for financial support during the course of this work.

References and Notes

(1) Davies, R. O.; Jones, G. O. *Adv. Phys.* **1953**, *2*, 370.
(2) Hodge, I. M. *J. Non-Cryst. Solids* **1994**, *169*, 211.
(3) Moynihan, C. T.; Macedo, P. B.; Montrose, C. J.; Gupta, P. K.; DeBolt, M. A.; Dill, J. F.; Dom, B. E.; Drake, P. W.; Esteal, A. J.; Elterman, P. B.; Moeller, R. P.; Sasabe, H. *Ann. N.Y. Acad. Sci.* **1976**, *279*, 15.
(4) Struik, L. C. E. *Physical Aging in Amorphous Polymers and Other Materials*; Elsevier: Amsterdam, 1978.
(5) Kovacs, A. J.; Aklonis, J. J.; Hutchinson, J. M.; Ramos, A. R. *J. Polym. Sci., Polym. Phys. Ed.* **1979**, *17*, 1097.
(6) Hodge, I. M.; Huvard, G. S. *Macromolecules* **1983**, *16*, 371.
(7) Hodge, I. M.; Berens, A. R. *Macromolecules* **1982**, *15*, 762.
(8) Gómez Ribelles, J. L.; Ribes Greus, A.; Díaz Calleja, R. *Polymer* **1990**, *31*, 223.
(9) Perez, J.; Cavaillé, J. Y.; Díaz Calleja, R.; Gómez Ribelles, J. L.; Monleón Pradas, M.; Ribes Greus, A. *Makromol. Chem.* **1991**, *192*, 2141.
(10) Hutchinson, J. M.; Ruddy, M. *J. Polym. Sci., Polym. Phys. Ed.* **1988**, *26*, 2341.
(11) Montserrat, S. *Prog. Colloid Polym. Sci.* **1992**, *87*, 78.
(12) Narayanaswamy, O. S. *J. Am. Ceram. Soc.* **1971**, *54*, 491.
(13) Scherer, G. W. *J. Am. Ceram. Soc.* **1984**, *67*, 504.
(14) Hodge, I. M. *Macromolecules* **1987**, *20*, 2897.
(15) Scherer, G. W. *J. Non-Cryst. Solids* **1990**, *123*, 504.
(16) Mijovic, J.; Nicolais, L.; D'Amore, A.; Kenny, J. M. *Polym. Eng. Sci.* **1994**, *34*, 381.
(17) Gómez Ribelles, J. L.; Monleón Pradas, M. *Macromolecules* **1995**, *28*, 5867.
(18) Gómez Ribelles, J. L.; Monleón Pradas, M.; Vidaurre Garayo, A.; Romero Colomer, F.; Mas Estellés, J.; Meseguer Dueñas, J. M. *Polymer*, in press.
(19) Cowie, J. M. G.; Ferguson, R. *Polymer Commun.* **1986**, *27*, 251.
(20) Gómez Ribelles, J. L.; Díaz Calleja, R.; Ferguson, R.; Cowie, J. M. G. *Polymer* **1987**, *28*, 2262.
(21) Cowie, J. M. G.; Ferguson, R. *Macromolecules* **1989**, *22*, 2307.
(22) Cowie, J. M. G.; Ferguson, R. *Polymer* **1993**, *34*, 2135.
(23) Adam, G.; Gibbs, J. H. *J. Chem. Phys.* **1965**, *43*, 139.
(24) Williams, G.; Watts, D. C. *Trans. Faraday Soc.* **1970**, *66*, 80.
(25) Gibbs, J. H.; DiMarzio, E. A. *J. Chem. Phys.* **1958**, *28*, 373.
(26) Miller, A. A. *Macromolecules* **1978**, *11*, 859.
(27) Rehage, G.; Brochard, W. In *The Physics of Glassy Polymers*; Haward, R. N., Ed.; Applied Science: London, 1973.
(28) Gómez Ribelles, J. L.; Monleón Pradas, M.; Vidaurre Garayo, A.; Romero Colomer, F.; Mas Estellés, J.; Meseguer Dueñas, J. M. *Macromolecules* **1995**, *28*, 5878.
(29) Meseguer Dueñas, J. M.; Vidaurre Garayo, A.; Romero Colomer, F.; Mas Estellés, J.; Gómez Ribelles, J. L.; Monleón Pradas, M. Results on styrene-acrylonytrile copolymer, submitted for publication.
(30) Montserrat, S.; Hutchinson, J. M.; Gómez Ribelles, J. L.; Meseguer Dueñas, J. M. Results on a fully cured epoxy resin, submitted for publication.
(31) Moynihan, C. T.; Easteal, A. J.; DeBolt, M. A.; Tucker, J. *J. Am. Ceram. Soc.* **1976**, *59*, 12.
(32) Tribone, J. J.; O'Reilly, J. M.; Greener, J. *Macromolecules* **1986**, *19*, 1732.
(33) Romero Colomer, F.; Gómez Ribelles, J. L. *Polymer* **1989**, *30*, 849.
(34) Hodge, I. M. *J. Non-Cryst. Solids* **1991**, *131−133*, 435.
(35) Nedler, J. A.; Mead, R. *Comput. J.* **1965**, *7*, 308.
(36) Angell, C. A. *J. Non-Cryst. Solids* **1991**, *131−133*, 3.
(37) Miller, A. A. *J. Polym. Sci., Part A2* **1968**, *6*, 1161.
(38) Wunderlich, B.; Bodily, D. M.; Kaplan, M. H. *J. Appl. Phys.* **1964**, *35*, 95.
(39) Chen, H. S.; Wang, T. T. *J. Appl. Phys.* **1981**, *52*, 5898.
(40) Privalko, V. P.; Demchenko, S. S.; Lipatov, Y. S. *Macromolecules* **1986**, *19*, 901.
(41) O'Reilly, J. M.; Hodge, I. M. *J. Non-Cryst. Solids* **1991**, *131−133*, 451.
(42) Prest, W. N.; Roberts, F. J., Jr., Hodge, I. M. In *Proceedings of the 12th NATAS Conference*; Buck, J. C., Eds.; NATAS: Williamsburg, VA, 1983; pp 119−123.
(43) Hutchinson, J. M. *Prog. Colloid Polym. Sci.* **1992**, *87*, 69.
(44) Saito, S.; Nakajima, T. *J. Appl. Polym. Sci.* **1959**, *2*, 93.
(45) Onogi, S.; Masuda, T.; Kitagawa, K. *Macromolecules* **1970**, *3*, 109.
(46) Karasz, F. E.; Bair, H. E.; O'Reilly, J. M. *J. Phys. Chem.* **1965**, *69*, 2657.
(47) Abu-Isa, I.; Dole, M. *J. Phys. Chem.* **1965**, *69*, 2668.
(48) Miller, A. A. *Macromolecules* **1970**, *3*, 674.

MA960336M